

Diverse receptive fields in the lateral geniculate nucleus during thalamocortical development

Sohail F. Tavazoie and R. Clay Reid

Department of Neurobiology, Harvard Medical School, 220 Longwood Avenue, Boston, Massachusetts 02115, USA

Correspondence should be addressed to R.C.R. (clay_reid@hms.harvard.edu)

Most models of thalamocortical development in the visual system assume a homogeneous population of thalamic inputs to the cortex, each with concentric on- or off-center receptive fields. To test this, we made high-resolution spatial maps of receptive fields in the developing ferret lateral geniculate nucleus (LGN). Developing receptive fields (RFs), had a variety of shapes: some concentric, others elongated (like adult cortical receptive fields) and some with 'hot spots' of sensitivity. These receptive fields seemed to arise from convergence of multiple retinal afferents onto LGN neurons. We present a Hebbian model whereby imprecise retinogeniculate connections help refine geniculocortical connections, sharpening both thalamocortical topography and perhaps orientation selectivity.

Early studies of the effects of visual deprivation demonstrated the essential role of sensory experience in the development of the highly specific connections from thalamus to visual cortex¹. Since then, the mechanisms underlying this refinement process have been extensively investigated, and models that attempt to explain it have been proposed^{2–6}. It is generally believed that during development, thalamic neurons compete for synapses onto cortical neurons. One basis for competition is the presence or absence of correlations among geniculate inputs, inherited from correlated activity between retinal ganglion cells^{7,8}. Correlations in activity between geniculate inputs, such as those between cells representing the same eye or cells of the same center type, are thought to be detected by cortical neurons and result in the strengthening of synapses of such inputs^{4,9–11}.

The receptive-field shapes of the geniculate inputs to cortex may also be important in thalamocortical development. Most models of thalamocortical development assume geniculate inputs to be a homogeneous pool of concentric, on- or off-center cells, similar to those found in the adult^{6,12,13}. Although their two-dimensional structure is not yet characterized, immature geniculate receptive fields get smaller during the first few weeks following eye opening in kittens¹⁴ and the first postnatal year in the monkey¹⁵.

The maturation of retinogeniculate connections is almost certainly the mechanism for the reduction of receptive-field size in the developing LGN^{16–18}. In the immature LGN, a large receptive field may result from the convergence of synaptic inputs from multiple ganglion cells onto a geniculate neuron¹⁹. The elimination or weakening of many such synapses during development would lead to a reduction in receptive-field size.

The final phase of retinogeniculate maturation overlaps with the critical period for thalamocortical development. In kittens, spatial receptive-field maturation in the LGN occurs during the first 2–3 weeks after eye opening¹⁴. The maturation of ocular dominance columns³ and orientation selectivity^{20–24} in visual cor-

tex occur during the first few weeks after eye opening in cats and ferrets. It is thus probable that imprecise connectivity from retina to LGN at this stage influences thalamocortical development

RESULTS

We recorded extracellularly from 112 neurons in layers A and A1 of the lateral geniculate nucleus of the ferret: 88 neurons in immature animals at postnatal day 31–55 (P31–P55) and 24 in adults. In addition, we recorded, in the optic tract, responses of five retinal ganglion cells from P37 and P39 animals. Eyes first open on postnatal day 30–34 in the ferret²⁵.

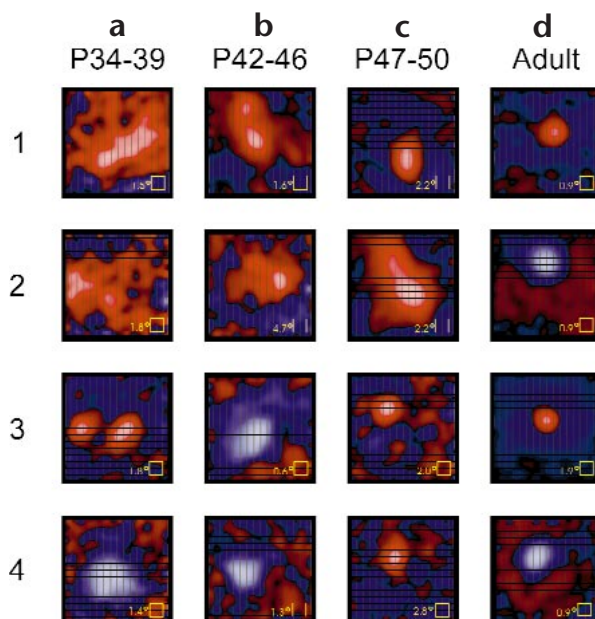
Spatial structure of developing geniculate receptive fields

For all cells studied, we mapped the receptive fields with a white-noise stimulus that consisted of 16×16 squares (pixels), each modulated in time by a binary temporal sequence²⁶. Receptive-field maps from LGN cells in adult ferrets qualitatively resembled those obtained in previous studies of the cat LGN²⁷: they were concentric and had antagonistic center/surround organization (Fig. 1d). Receptive fields of geniculate neurons in immature ferrets, however, had a variety of shapes (Fig. 1a–c). Many cells at the youngest ages studied had large, roughly circular receptive fields (Fig. 1a4). Other cells from young (P34–P39; Fig. 1a1–a3) and intermediate aged (P42–P47; Fig. 1b1 and c2) animals had elongated receptive fields. Some developing receptive fields had isolated 'hot spots' of high sensitivity (Fig. 1a3 and b1). Although non-concentric receptive fields were mapped from developing animals older than P47, a larger number of cells at these ages had more adult-like receptive fields (concentric, center/surround organization; Fig. 1c3 and c4).

Trial-to-trial robustness of receptive-field structure

To ensure that the receptive fields we mapped belonged to single cells, great care was taken to verify the quality of the recordings. Only well-isolated action potentials, as assessed by online

Fig. 1. Diversity of receptive-field shapes in the developing ferret LGN. Sixteen geniculate receptive fields mapped at various developmental ages. Postnatal ages are labeled at the top of each column; each panel corresponds to a separate receptive field. Receptive-field maps were calculated from extracellular responses to a white-noise (*m*-sequence) stimulus by a reverse-correlation method²⁶. Red regions in the receptive-field maps correspond to areas excited by bright stimuli (on) and blue to dark stimuli (off). Brightness corresponds to the strength of response. Black grid indicates pixel size; yellow squares indicate degrees of visual angle. Some receptive fields were oriented (**a1–a3**, **b1**, **b3** and **c2**), and some had spatially isolated 'hot-spots' (**a2**, **a3**, **b1**). Other cells at the youngest ages had large, roughly concentric receptive fields (**a4**, **b4**). Adult receptive fields (**d**) were concentric and had antagonistic center-surround organization²⁷.



and offline spike cluster analysis, were used in this study. The presence of absolute and relative refractory periods in a cell's spike train was an additional requirement for a cell to be classified as a single unit. For every cell, the refractory period was deduced from the spike train's autocorrelogram, which indicates the frequency with which any two spikes occur at a given interval. In all but eight cases, only the largest spike recorded on an electrode was used; when a second spike from the same electrode was used, particular care was taken in assessing the waveform and the autocorrelogram.

We also examined whether features of receptive-field maps from immature animals were reproducible. We were able to record the responses of some neurons for sufficiently long periods to allow several repeats of the white-noise stimulus (which lasted either 8 or 16 minutes, see Methods). The maps obtained from three separate eight-minute runs are shown for a P45 cell (Fig. 2a). These receptive-field maps were extremely similar. We also show the waveform of the action potential (Fig. 2b) and the autocorrelogram (Fig. 2c). The spike was very well separated from the noise, and there was a 4-ms refractory period.

For other neurons, we were unable to record over multiple repeats of the white-noise stimulus. In this case, we divided the responses into eighths of the entire stimulus duration (one or two minutes each) and compared the receptive fields obtained from these shorter epochs. As seen for a P47 cell, the receptive fields obtained from each one-minute segment of the stimulus (Fig. 2d, black outlines) were grossly similar to the receptive field obtained from the entire stimulus (Fig. 2d, dashed outline). Thus the structure of the measured receptive field was stationary over short time scales and did not result either from measurement noise or from eye movement during the stimulus period. The

waveform of the action potential (Fig. 2e) and the autocorrelogram (Fig. 2f) confirm that the cell was well isolated, and the spike train had a 2.8-ms refractory period.

Maturation of receptive-field size

Although the maps obtained with the two-dimensional white-noise stimulus had a great degree of spatial detail, they could also be used to assess gross features, such as the size of the receptive-field center. Previous studies of the kitten¹⁴ and monkey¹⁵ LGN, using sinusoidal gratings or spots of light as stimuli, show that receptive fields become smaller in the early postnatal period. We quantified the receptive-field size in the ferret LGN by fitting each receptive-field map to a two-dimensional Gaussian. When plotted as a function of age, the diameter of the Gaussian fits (2σ , see legend) clearly decreased between P30 and adulthood (Fig. 3, circles). Receptive fields were largest during early development ($<P45$) and became progressively smaller later in development ($>P45$) and in the adult (early versus late, $p < 0.001$, Mann-Whitney test; late versus adult, $p < 10^{-5}$). In total, 55% (47 of 86) of developing LGN cells had receptive fields larger than the largest adult receptive field ($2\sigma = 2.6^\circ$). Additionally, the receptive fields of retinal ganglion cells mapped from optic tract responses in P37 and P39 animals ($>35^\circ$ eccen-

Fig. 2. Reproducibility of fine receptive-field structure. (a) Three receptive-field maps obtained from three successive eight-min repeats of the white noise stimulus for a P45 cell. Each contour corresponds to a step equal to 10% of the peak response. (b) Waveform (black curves) of the action potential for the neuron in (a); the spike was well isolated from the noise (gray curves). (c) Auto-correlogram of the same spike train used to construct the receptive field in (a). A 4-ms refractory period confirmed isolation of a single cell (total spikes, 3473). (d) Receptive-field maps of a P47 cell. Dashed box, receptive field from an eight-min stimulus run. Black boxes, eight consecutive one-min segments of the stimulus. (e) Spike waveform and (f) autocorrelogram (total spikes, 7347) for the cell in (d).

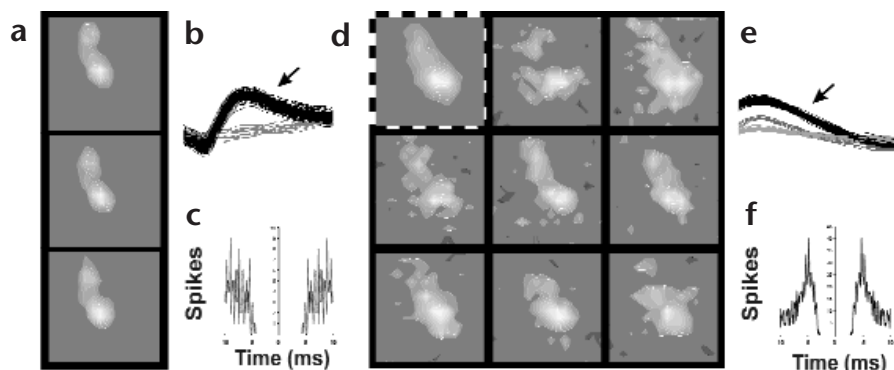
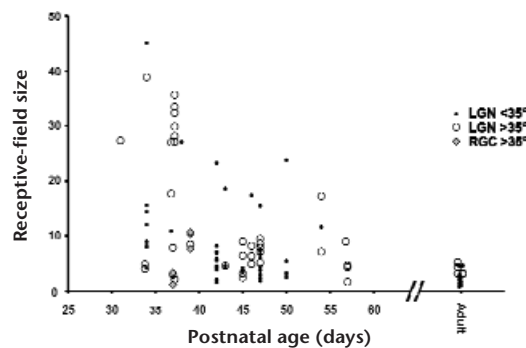


Fig. 3. Receptive-field center diameter of LGN cells, plotted as a function of age. The diameters tended to decrease between P30 and adulthood. Filled circles, eccentricity $<35^\circ$; open circles, eccentricity $>35^\circ$. Gray diamonds, data from five retinal ganglion cells, eccentricity $>35^\circ$. The centers of the spatial receptive fields were fit to symmetric two-dimensional Gaussian functions (diameter, 2σ). Data from each age correspond to a single experiment, except for P34, P37, P57 and adult. For these four ages, data points from each experiment are offset slightly to allow separate assessment.



tric) were found to be smaller than most geniculate receptive fields of comparable ages (Fig. 3, diamonds). It is also important to note that the decrease in size with age did not depend on differences in eccentricities between the different samples (analysis not shown); in particular, even the adult cells that were $>35^\circ$ eccentric had receptive fields significantly smaller than most cells of $<35^\circ$ at early time-points.

One- and two-Gaussian receptive-field fits

In the adult retina and LGN, receptive-field centers are circularly symmetric and well represented as a single two-dimensional Gaussian (but see refs. 28, 29). In developing animals, however, we found some receptive-field centers had asymmetric shapes, as illustrated above (Fig. 1). For a number of these LGN cells from developing ferrets, we found that the receptive-field center (Fig. 4a, left column) was better fit by two Gaussians of the same sign (Fig. 4a, middle column) than by a single Gaussian (Fig. 4a, right column). By comparison, receptive-field centers in the adult LGN (Fig. 4b, left column) were adequately fit by a single Gaussian (Fig. 4b, right column), with little improvement when fit with two Gaussians (Fig. 4b, middle column).

One interpretation of these results is that the part of the receptive field fit by the second Gaussian in some immature geniculate receptive fields represents input from one or more nearby

retinal ganglion cells. With further development, the additional inputs might be eliminated to yield the adult receptive fields, which closely resemble those of single retinal afferents^{27,30,31}. Many cells from the youngest animals (Fig. 1a4), however, had very large, roughly circular receptive fields that were well modeled by a single Gaussian. These cells might receive numerous inputs from different ganglion cells, resulting in smoother, roughly circular receptive fields.

Alternatively, two other factors might have caused the irregular receptive-field shapes (Fig. 4a, left column) observed in the developing LGN: either the optics of immature eyes may have distorted the stimulus projected onto the retina, or ganglion cells may have irregular receptive fields that are relayed to the LGN. To rule out these possibilities, we recorded from the axons of retinal ganglion cells in the optic tract of two young animals (P37 and P39). The receptive-field centers of these retinal ganglion cells (Fig. 4c, left column) were adequately fit by a single Gaussian (Fig. 4c, right column); the fit of these receptive fields, like those of adult cells, was not improved through the use of two Gaussians (Fig. 4c, middle column).

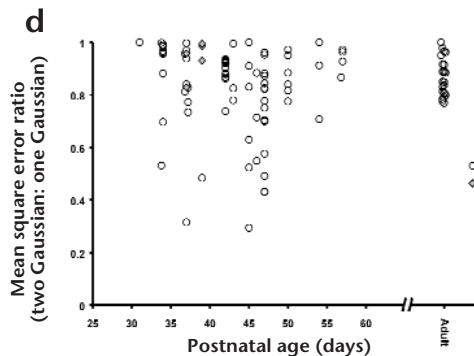
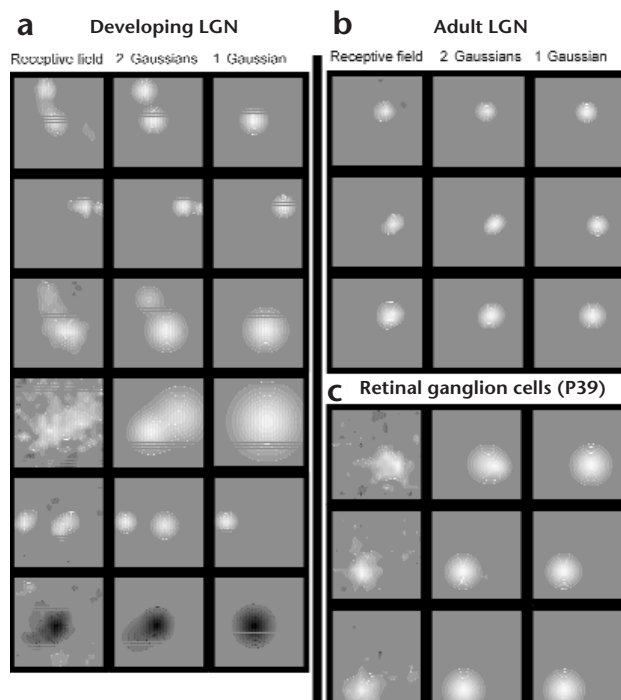


Fig. 4. Many developing receptive-field centers are much better represented as two Gaussians than one, whereas adult and ganglion-cell receptive-field centers are adequately represented by one Gaussian. (a–c) Left columns, contour plots of receptive-field centers. Middle columns, fits of the same receptive fields using two symmetric two-dimensional Gaussians. Right columns, fits to one symmetric two-dimensional Gaussian. (a) Geniculate cells from P34–P47. (b) Adult geniculate cells. (c) P39 retinal ganglion cells. Gray grid indicates 1/2 pixel size; data interpolated for Gaussian fits. (d) The ratio of the mean square error for the two-Gaussian fit over the one-Gaussian fit, plotted as a function of age, as in Fig. 3. Lower ratios correspond to cells that were better fit with two Gaussians. Open symbols, LGN neurons; gray diamonds, ganglion cells. In adult geniculate cells, the ratios ranged from 0.77 to 1 (mean, 0.87; median, 0.87). Between ages P34 and P47, the ratios spanned a far broader range (0.29–1; mean, 0.81; median, 0.87).

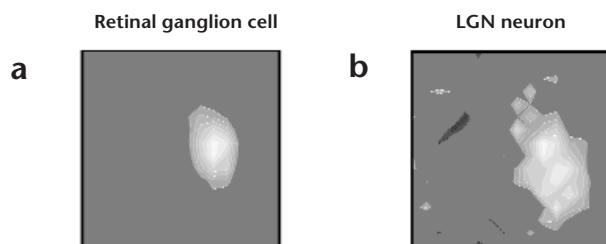


Fig. 5. The relationship between an immature LGN neuron and one of its ganglion-cell inputs. Receptive-field maps of a ganglion cell constructed from an S-potential recording (**a**) and a spatially overlapped LGN neuron recorded on the same electrode (**b**) in a P45 animal. The ganglion cell only accounts for the top half of the geniculate receptive field.

Thus two factors argue against poor optics or retinal immaturity as the cause of immature geniculate receptive-field shapes¹⁹: first, these ganglion-cell receptive fields were smaller relative to most comparably aged geniculate receptive fields (Fig. 3) and, second, their shapes were adult-like (Gaussian; Fig. 4c). If geniculate receptive fields were actually small and homogeneous, but seemed inhomogeneous because of poor optics, then the retinal receptive fields would seem similarly distorted. Further, often in the same animal—and, in rare instances, during simultaneous recording from two cells (Fig. 1c1 and c2)—we would encounter both homogeneous and inhomogeneous geniculate receptive fields.

We next sought to quantify the degree to which a second Gaussian provided a better fit to the receptive-field data. For each cell, we calculated the mean square error of the fit (see Methods) for both the single-Gaussian model and the double-Gaussian model. The ratio of these mean square errors—the double-Gaussian error over the single-Gaussian error—gives a good measure of the improvement of fit with the second Gaussian. A ratio near 1.0 implies that the two Gaussians are no better than one in describing the receptive field. A lower ratio (<1.0) implies that the two-Gaussian model provides a better fit over the one-Gaussian model. We plotted the ratio of the mean square errors versus age (Fig. 4d) for LGN cells in the developing ferret. On the same plot, we indicated this ratio for five retinal ganglion cells from P37 and P39 ferrets and 24 cells from adult ferrets. In adult geniculate cells, ratios ranged from 0.77 to 1 (mean, 0.87; median, 0.87; s.d., 0.076). Note that between ages P34 and P47, the ratios spanned a far broader range (0.29–1; mean, 0.81; median, 0.87; s.d., 0.18). In particular, 28% (18 of 64) of these cells had ratios <0.77 (the lowest value in the adult). One could argue that the difference we observed between adult and developing receptive fields was due to the noisier receptive-field maps found during development, as the spike rates are lower^{14,15}. Indeed, the median number of spikes evoked by the white-noise stimulus from developing LGN cells (1023) was lower than the median spike count from adult cells (5283). We therefore did a control in which we produced receptive-field maps with only 500 spikes from each adult cell (and the immature ganglion cells). When we analyzed the error the two-Gaussian versus one-Gaussian fits for these new receptive fields, the results (data not shown) were indistinguishable from those obtained with all of the spikes.

Receptive-field overlap for a retina–LGN pair

The considerable difference between retinal and geniculate receptive fields during development is probably caused by convergence of multiple ganglion cells onto single geniculate targets. In the

adult, there are usually only one or two strong ganglion-cell inputs to a geniculate cell, and the receptive-field centers of pre- and postsynaptic cells are quite similar and spatially overlapped. This has been shown directly by recording simultaneously in retina and LGN^{30,31}. It has also been shown with a single electrode in the LGN, which can sometimes record the action potential of the LGN cell along with the synaptic potential (S-potential) of a dominant retinal input²⁷. The S-potential is an extracellular record of the current entering the postsynaptic cell due to the activation of a single retinal fiber. We show an example of such an S-potential recording in a P45 ferret (Fig. 5). Oscilloscope traces triggered by the S-potential revealed that the geniculate cell often fired immediately after the S-potential. This observation, along with more quantitative cross-correlation analysis, confirmed that the retinal ganglion cell associated with the S-potential provided monosynaptic input to the geniculate neuron. The receptive-field center of the ganglion-cell input (Fig. 5a) was smaller than the geniculate receptive-field center (Fig. 5b) and overlapped only the top half. Therefore, at least half of the geniculate receptive field must derive from one or more additional ganglion cells. Importantly, the retinal and geniculate receptive fields are more dissimilar than any retinogeniculate pair observed in the adult cat³¹.

Elongation of developing geniculate receptive fields

So far, we have demonstrated that receptive-field centers in the developing ferret were both larger and more inhomogeneous than in the adult. We next investigated the degree of elongation of developing geniculate receptive fields. A common measure of the degree of elongation of a cortical receptive field (or a subregion of a receptive field) is the aspect ratio, or the ratio of length to width. To quantify aspect ratios for geniculate cells, we fit the receptive-field centers to single elliptical Gaussians. This was only loosely related to our previous analysis; many of the receptive fields that were well fit by two circular Gaussians were elongated (for example, Fig. 4a), but the goodness of the two-Gaussian fit did not predict the aspect ratio (see Methods).

In the adult, aspect ratios ranged from 1.03 to 2.66 (Fig. 6; mean, 1.62; median, 1.58). This range was similar to values reported for the adult cat LGN²⁹ (mean, 1.26) and retinal ganglion cells³² (mean, 1.23). In the developing ferret, we found

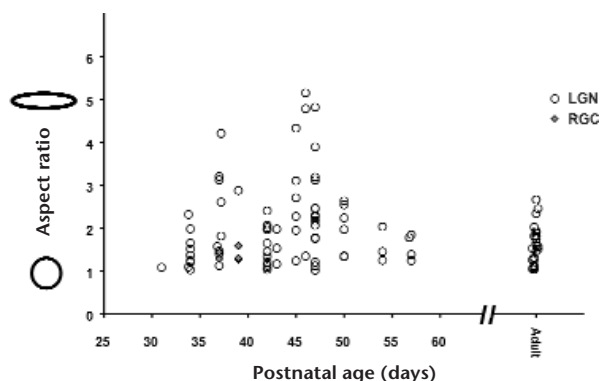


Fig. 6. Receptive-field elongation. Aspect ratios (length:width) of geniculate receptive fields plotted as a function of age, as in Fig. 3. Open circles, LGN cells; gray diamonds, retinal ganglion cells. In all but two cases (see Methods), the aspect ratio was taken as the length:width ratio of the best two-dimensional elliptical Gaussian fit. Adult geniculate aspect ratios ranged from 1.03–2.66 (mean, 1.62; median, 1.58). In developing animals, aspect ratios as great as 5 were found (range, 1.01–5.15; mean, 2.0; median, 1.77).

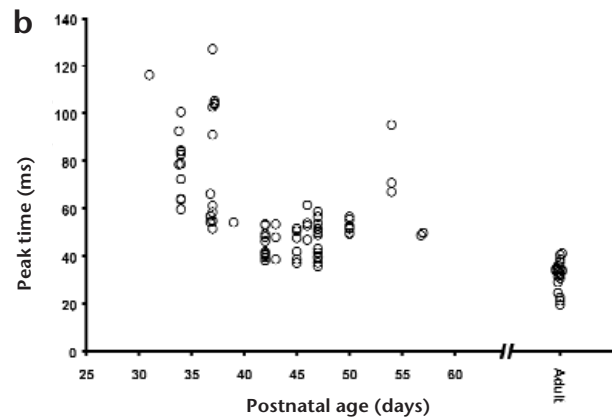
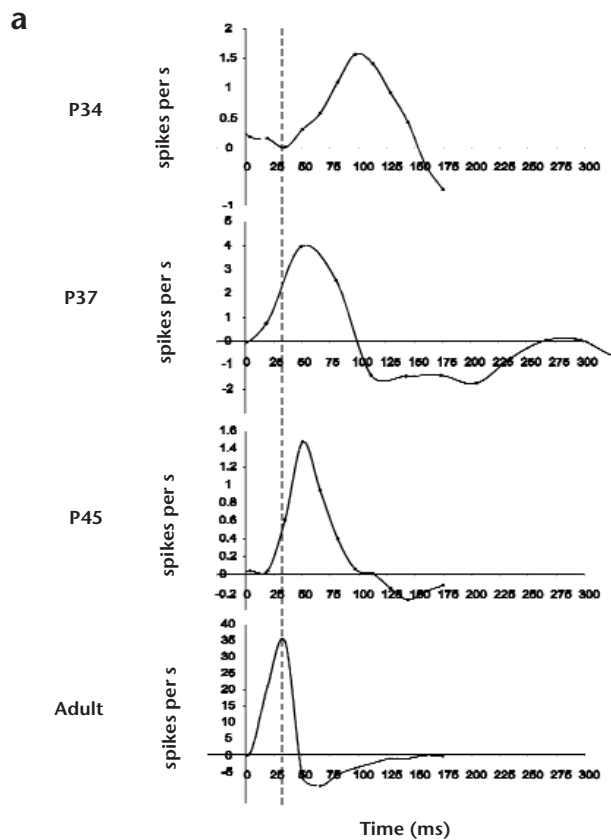


Fig. 7. Maturation of geniculate response timing. Temporal response functions (see Methods) of four on-center cells at various developmental ages. For each cell, response amplitude is plotted as a function of time after the stimulus.

aspect ratios as great as 5 (range, 1.01–5.15; mean, 2.0; median, 1.77). As a population, receptive fields in the developing geniculate (P37–P50) were more elongated than adult receptive fields ($p < 0.025$); 17% (13 of 77) were more elongated than the most elliptical adult receptive field. They were also, on average, more elongated than developing ganglion-cell receptive fields. Early in development ($<P45$), however, receptive fields as a population were less elongated than later in development ($>P45$; $p < 0.025$). Orientation-biased responses to moving bars or gratings are also reported in the LGN of the adult cat^{28,29}, consistent with our finding of moderate aspect ratios.

Maturation of temporal responses

A complete description of a visual neuron's receptive field requires an examination of the cell's temporal as well as spatial response properties. So far, we have presented the spatial receptive fields obtained by considering only one delay between stimulus and response (the delay that produced the largest response). The white-noise method, however, produces a receptive-field map for any delay between stimulus and response. The evolution of these spatial receptive fields—the temporal response function (related to the impulse response)—can be represented as the sum of the responses evoked by all of the pixels in the receptive-field center³¹.

Temporal response functions of LGN cells from younger animals were broader and peaked later than temporal response functions from adult LGN cells (Fig. 7a). The peak response time decreased consistently as a function of age (Fig. 7b). Response latency (assessed through different means and with different stimuli) decreases during development in the kitten¹⁴ and monkey¹⁵. At slightly later developmental stages in kittens (weeks 4 and 8, which corresponds to roughly P50 and P79 in the ferret²⁵), temporal response functions are also slower than in the

adult³³. Our findings suggest that temporal responses from LGN cells recorded at around the time of eye opening were even broader and had significantly slower peak times than temporal responses at these later ages. These reductions in response times probably reflect retinal maturation, the complete myelination of the optic nerve and the presence of more robust retinogeniculate synapses in the adult. Interestingly, at the earliest time points in development (Fig. 7b; P34, P37), response-peak times varied significantly among LGN cells. This bears on models of cortical coincidence detection, because stimulus-induced action potentials in nearby geniculate cells could have very different arrival times in cortex.

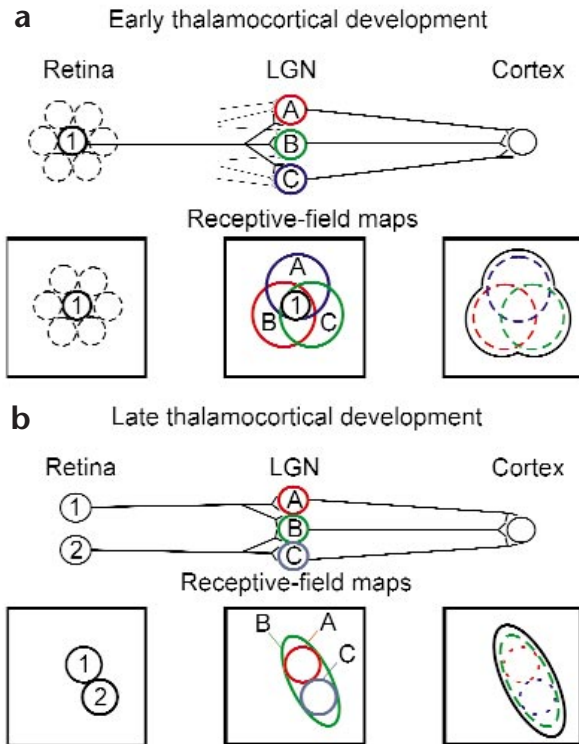
Our findings suggest that receptive fields in the developing LGN are diverse—some concentric, others inhomogenous and/or oriented—and that they arise from the convergence of multiple retinal inputs onto single geniculate neurons.

DISCUSSION

We used white noise and reverse correlation analyses to map the two-dimensional spatial structures of geniculate receptive fields throughout visual system development in the ferret. Previous studies in the cat¹⁴ and monkey¹⁵ show that geniculate receptive fields tend to decrease in size during early postnatal development. Our results confirmed and extended these results in the ferret by examining not only the size of receptive fields, but also their shapes at high resolution.

At all ages from P31–P55, geniculate receptive fields had diverse shapes. Some receptive fields mapped in the youngest animals were large and roughly circular. Other cells in the first few weeks after eye opening had non-concentric receptive fields; some geniculate receptive fields were elongated, resembling cortical receptive fields, and some had spatially isolated hot spots of sensitivity. Receptive fields of retinal ganglion cells from young animals were smaller and concentric. This suggests that diverse receptive-field shapes in the immature LGN result from the convergence of synapses from multiple ganglion cells onto single geniculate neurons.

Cortical layer 6 and the perigeniculate nucleus also provide visual input to the LGN, but for several reasons, we believe that the unusual receptive-field shapes we observed during development were not influenced by these sources. In the adult, recep-



tive-field centers are determined primarily by their retinal afferents^{30,31}. Feedback may affect the surround and other more subtle aspects of receptive fields, such as length tuning³⁴, but it does not affect the spatial structure of the center. The retina provides the driving input to the LGN, whereas feedback provides a more modulatory input (for review, see ref. 35). In addition, the unoriented white-noise stimulus we used here is far more effective in driving retinal cells than in driving layer 6 cortical neurons (R.C. Reid, J.-M. Alonso and W.M. Usrey, unpublished observations), and would thus further accentuate the retinal influence. The inhibitory inputs from the perigeniculate are more poorly understood; the diffuse inhibition they provide is unlikely to have affected the receptive-field center.

Relationship to anatomical maturation

The structural basis for the receptive-field maturation we observed was probably the elimination of retinal ganglion-cell synapses onto inappropriate geniculate targets. The axonal arbors of retinal ganglion cells decrease in terminal-field width during the weeks after eye opening (at least for X cells¹⁷, the predominant cell type in the ferret A layers). They also undergo more subtle structural changes—such as the loss of growth-cone-like structures from axonal arbors and the thickening of terminal swellings—during this same period¹⁶.

Although retinogeniculate terminal arbors remodel and mature during the weeks following eye opening^{16,17}, their gross anatomical refinement should not be equated with the changes in convergence that we see physiologically. To reconcile the anatomical and physiological changes that occur during the weeks following eye opening, it is useful to draw the distinction between gross morphological divergence/convergence and functional divergence/convergence. We define functional divergence from retina to LGN as the number of LGN cells that receive synaptic input from a given ganglion cell; convergence is the number of retinal inputs that synapse onto a single target. Morphological

Fig. 8. The convergence/divergence model of thalamocortical development. (a) During early thalamocortical development, the convergence of inputs from multiple ganglion cells results in large geniculate receptive fields. LGN cells A–C each receive convergent inputs from three ganglion cells. (Only one input is shown.) Ganglion cell 1 diverges and synapses onto all three LGN cells. The spontaneous or stimulus-dependent firing of cell 1 would synchronize the activities of cells A–C and make them, based on Hebbian mechanisms, more likely to connect to the same cortical target. Cortical topography is thus tightened by the grouping of LGN cells with nearby receptive fields. (b) At a later stage, when divergence from retina to LGN is more limited, each geniculate neuron receives inputs from a few ganglion cells. Ganglion cells 1 and 2 converge onto geniculate cell B, which has an elongated receptive field. Geniculate cells A and C have circular receptive fields, as they receive their dominant input from ganglion cells 1 and 2, respectively. The divergence of ganglion cell 1 would synchronize the activities of LGN cells A and B; ganglion cell 2 synchronizes the activities of LGN cells B and C. If a cortical neuron received input from cell B, then any connections from cells A and C would increase in strength through a Hebbian mechanism. In this way, geniculate neurons can be grouped together, through retinal divergence and convergence, to construct or fine-tune oriented cortical receptive fields.

divergence can be defined as either the number of terminal boutons or the extent of the axonal arbor.

The distinction between morphological and functional divergence/convergence is well illustrated by the mature LGN. In the cat, retinal X-cell arbors have on the order of 500–1,000 boutons, which ramify over more than 100 geniculate relay neurons; conversely, each geniculate relay neuron has dendrites that overlap with more than 50 retinal axons^{17,36}. Although these morphological features would allow for each relay neuron to receive inputs from many different afferents, only a few very specific connections are made onto each cell. This specificity is seen both physiologically^{30,31} and in ultrastructural studies³⁶.

During development, therefore, a decrease in functional divergence need not coincide with a change in axonal morphology. One could imagine that, early in development, a single ganglion cell may form 1,000 synapses onto 20 geniculate cells. This same ganglion cell in the adult may still form 1,000 synapses but now onto only 5 geniculate cells. The same principle holds for synaptic convergence, as the number of pre- and postsynaptic cells is constant during this period (discussed below). Significant changes in functional divergence/convergence could thus occur in the absence of changes in the gross morphology of axonal arbors.

At the earliest ages we studied, large and somewhat circular receptive fields probably arise from the functional convergence of many ganglion cells onto a geniculate target. These somewhat coarse connections are most probably established by waves of spontaneous retinal activity occurring during the early postnatal period⁸. At later stages, as synapses are eliminated from some of the inappropriate targets and formed onto a smaller number of targets, some geniculate cells would have elongated or inhomogeneous receptive fields. Our surprising finding that some geniculate receptive fields had spatially offset 'hot spots' (Fig. 1a3 and b1) suggests that, during development, a few ganglion cells may synapse strongly onto a target, whereas an interposed ganglion cell may not.

Developmental implications: transient LGN synchrony

Our findings have several implications for the development of thalamocortical connections. Most simply, developing cortical

neurons will inherit the diverse features of geniculate receptive fields, in particular, their orientation. This is a variant of developmental models in which the weaker orientation biases observed in the adult LGN serve as ‘nuclei’ around which cortical orientation selectivity is constructed²⁸.

A more interesting developmental mechanism is based on synchronous activity in the thalamus, caused by common retinal input. By postnatal day 6 in the ferret, the adult number of ganglion cells is established⁴¹, and by P22, the LGN attains its adult structure⁴². Therefore, because we found strong indirect evidence that retinogeniculate convergence during these periods is considerably greater than in the adult, retinogeniculate divergence should also be commensurately greater (assuming that all ganglion cells have a comparable number of outputs, and all geniculate cells a comparable number of inputs). This divergence should synchronize the activity of ensembles of LGN cells and result in the strengthening of their connections to common cortical targets by Hebbian mechanisms. This form of synchrony occurs in the adult between each pair of LGN cells that receive common input from a given ganglion cell^{37–39}. Such synchrony should be far more prevalent during development, because retinal divergence is more extensive.

Correlations within the retina (and thus the LGN) are proposed to be important in the development of visual cortex^{6,8,40}. The mechanism we propose is related, but fundamentally differs in key aspects. Slow waves of activity are proposed to be involved in development of eye segregation and topography early in development⁸. Later in development, faster correlations in the retina are proposed to function similarly⁶. These faster correlations are caused by common input to ganglion cells from overlapping pools of either bipolar or amacrine cells (as studied in the mature retina⁴⁰). The form of correlation we propose is also due to common input, but it is present only transiently during development. It is also much faster (~1 ms in the adult^{37,38}) than the correlations seen in the developing retina. The most important point is that the imprecise connections to the LGN—which cause the correlations—are refined at the same time as the connections from LGN to visual cortex.

In light of our findings, we propose a model of thalamocortical development based on divergence and convergence of retinthalamic connections (Fig. 8). Although this model applies to cat and ferret, two differences relating to the physiology of layer 4 must be noted: in the ferret, there is on–off segregation (which certainly must affect some models of developing orientation selectivity⁶), and the percentage of oriented cells in layer 4 is lower in the ferret²².

Transient synchrony and topographic refinement

During the early stages of thalamocortical development, some geniculate receptive fields are large, presumably due to the convergence of inputs from many ganglion cells. For simplicity, we depict LGN cells that receive convergent inputs from only three retinal ganglion cells (Fig. 8a), although the actual numbers are probably much higher. Each retinal ganglion cell, therefore, diverges onto three LGN cells. The spontaneous or stimulus-dependent firing of cell 1 would synchronize the activities of cells A–C³⁸. These three geniculate cells could synchronously drive a common cortical target and thus, based on Hebbian mechanisms^{9,10}, would strengthen their connections to this target.

The continued action of this mechanism will refine the geniculocortical connections, driven by the refinement of the retinogeniculate connections. As geniculate receptive fields become progressively smaller, only those that received common retinal

inputs would maintain their strong connections to a given cortical target. Importantly, because eye segregation is complete in the LGN by this stage, only those geniculate cells receiving input from a given eye would be synchronized. Thus, thalamic synchrony could potentially sharpen ocular dominance columns as well.

A geniculate scaffolding for orientation refinement

A similar mechanism is best illustrated with an example from a slightly later stage in development, when orientation selectivity is maturing in visual cortex (Fig. 8b). At ages P42–P50, for example, we found a mixture of elongated and concentric receptive fields, some quite small (Fig. 1c1 and c2, recorded simultaneously; Fig. 6). For simplicity, we depict the convergence of two ganglion cells (1 and 2) onto geniculate cell B, which consequently has an elongated receptive field (Fig. 8b). Geniculate cells A and C have circular receptive fields, as they receive their dominant input from ganglion cells 1 and 2, respectively. The divergence of ganglion cell 1 would synchronize the activities of LGN cells A and B. Similarly, the divergence of ganglion cell 2 would synchronize the activities of LGN cells B and C. If a cortical cell received input from cell B, then any connections from cells A and C would increase in strength through a Hebbian mechanism. Thus cell B could act as a scaffolding upon which a cortical neuron could strengthen inputs with colinear receptive fields, even though these inputs need not be correlated with each other.

In this way, geniculate neurons can be grouped together, through synchrony derived from retinal divergence, to finely tune oriented cortical receptive fields. Because there are ~2.5 geniculate cells for each ganglion cell (at least in the cat⁴³), and roughly 2 ganglion cells of a given center type cover each point of the retina⁴⁴, multiple orientations can be represented for each portion of visual space.

At a later point during development, Hebbian plasticity at thalamocortical synapses would cease, and the set of geniculate cells connected to a cortical cell would become fixed. For instance, in the example given here (Fig. 8b), the oriented input from cells A and C would persist even at a later stage, when the receptive field of cell B was not itself elongated. We believe that this is a realistic assumption, because synapses in visual cortical slices become significantly less susceptible to LTP as the critical period comes to an end⁴⁵.

This sort of model would require that oriented geniculate receptive fields (the scaffolding) impose a similar orientation on their cortical targets. To test this idea, the critical experiment would be to record simultaneously from oriented cortical and geniculate neurons during development (as in ref. 46) and determine whether oriented geniculate neurons connect preferentially with cortical neurons with similar orientations.

Our model provides a mechanism for the fine tuning of cortical receptive fields during development. An interesting question that still remains is how the original orientation map is set up. Although we did not characterize the receptive fields of geniculate cells before eye opening, oriented receptive fields were seen in the LGN within a day of eye opening and are probably present in the LGN earlier, before orientation maps are present in visual cortex²³. Thus the above mechanism (Fig. 8b) might actually be involved in setting up the orientation map as well. Our model, however, cannot be solely responsible for setting up the orientation map, as it does not account for the smoothness of the map. It is probable that such gross order in cortical maps is set up through other correlation-based mechanisms^{6,12,13} or genetic/molecular cues^{24,47} present at an earlier age (reviewed in ref. 5).

These two aspects of our proposed developmental mechanism—topographic refinement (Fig. 8a) and orientational scaffolding (Fig. 8b)—are not necessarily meant to represent discrete stages in development; they could both operate simultaneously. Certainly, receptive fields, as a population, are largest early in development (<P45) and become progressively smaller later in development (>P45) and in the adult (Fig. 3). Although receptive fields are most elongated in later development (>P45), they are somewhat elongated even in early development (although the difference between early development and the adult is not statistically significant; $p = 0.44$; Fig. 6).

In keeping with experimental evidence, our model does not require visual experience for the refinement of fine thalamocortical topography or cortical orientation selectivity^{2,24,48}. Instead, connections from the second to third stage (LGN to visual cortex) emerge as a result of the transient grouping of neurons through imprecise, divergent connections from the first to the second stage (retina to LGN). The ‘first’ stage in such a scenario need not be in the periphery, but could be from any source in the nervous system. Such a three-stage mechanism could have broader implications for the development of fine-scale topography or the emergence of order in circuits throughout the brain.

METHODS

Animal preparation. All surgical and experimental procedures conformed to NIH and USDA guidelines and were carried out with the approval of the Harvard Medical Area Standing Committee on Animals. We used 18 ferrets weighing 80–800 g and aged P31–P57 in this study. Additionally, we used four adult female ferrets. Our surgical procedures were carried out as previously reported³¹, with a few modifications for immature animals. Surgical anesthesia was induced with ketamine (25 mg per kg, intramuscular; Fort Dodge Animal Health, Fort Dodge, Iowa) and xylazine (2 mg per kg, intramuscular; Fermenta, Kansas City, Missouri). We cannulated the external jugular vein and administered continuous anesthesia (thiopental sodium 5 mg per kg per h, supplemented as needed; Abbott, North Chicago, Illinois) and the loading dose of paralytic (vecuronium bromide, 0.2 mg per kg; after completion of surgery). Maintenance paralytic (vecuronium bromide, 0.2 mg per kg per h; Organon, West Orange, New Jersey) was administered i.p. The cornea were protected with contact lenses 4 mm in diameter (base curvature, 280; Platt, Mount Vernon, Ohio). Proper depth of anesthesia was ensured throughout the experiment by monitoring the EEG for changes in slow-wave/spindle activity, by monitoring the EKG and expired CO₂ for changes associated with a decrease in the depth of anesthesia, and by testing for responses to toe pinch.

At the end of each experiment, animals were given a lethal dose of sodium pentobarbital (50 mg per kg). For some cases ($n = 12$), electrode tracks and lesions (made during the experiment by passing 4–5 μ A current for 4 s) were reconstructed from 50 μ m-thick sections stained with thionin. In all these cases, electrode tracks went through the LGN and lesions fell within the A layers.

Electrophysiological recordings and visual stimuli. Recordings were made from neurons in the LGN with tungsten in glass electrodes (Alan Ainsworth, London). Spike waveforms were digitized and saved to disk on a PC running Discovery software (Datawave, Longmont, Colorado). Spike isolation was confirmed with off-line analysis of the waveforms and by the presence of a refractory period, as inferred from autocorrelation plots.

Because the more dorsal C laminae were encountered first in each penetration, the more ventral A laminae were easily distinguishable. Neurons in the A laminae were distinguished from other visually responsive neurons (in the medial interlaminar nucleus, perigeniculate nucleus) by four criteria: their receptive fields were smaller (even in developing animals), their responses were more robust, receptive fields alternated between on- and off-center in the sublaminae of layers A, A1 (ref. 49) and they were monocularly driven.

Receptive fields of geniculate neurons were mapped by reverse correlating single-unit extracellular responses to pseudorandom spatiotemporal white-noise stimuli (m-sequences²⁶). The stimulus was a 16×16 grid of black and white squares (pixels) created with an AT-Vista graphics card (Truevision, Indianapolis, Indiana) running at a frame rate of 128 Hz. The stimulus of length 32,767 was updated every 2 or 4 frames (total time, ~8 or ~16 min). The stimulus program used subroutines from a runtime library, YARL, written by Karl Gegenfurtner. The mean luminance of the stimulus monitor was either 10 or 80 candelas per m². Pixels were small enough (0.3°–2.3°) to map receptive fields with a reasonable amount of detail. In almost all cases, the receptive-field center was at least four pixels across. To assess the time course and magnitudes of the response, it was necessary to identify the pixels in the receptive-field center. The center pixels were defined as all pixels that had the same sign (on or off) as the strongest pixel, were 2.0 standard deviations above the baseline noise and formed a contiguous region. The temporal response function was obtained by summing the responses from all the center pixels for each delay between stimulus and response³¹. As with young kittens¹⁴, it was difficult to classify X cells versus Y cells at these very early ages. In the adult ferret LGN, the great majority of cells encountered (87%) electrophysiologically in the A layers are X cells⁵⁰.

Gaussian models of the spatial receptive fields. The centers of the spatial receptive fields were fit to three different models, a single, symmetric (round) two-dimensional Gaussian, two symmetric Gaussians and a single oriented, elliptical Gaussian. The symmetric two-dimensional Gaussian is given by the function,

$$A e^{-[(x-x_0)^2 + (y-y_0)^2] / \sigma^2},$$

where A is the amplitude, x_0 and y_0 the coordinates of the center of the receptive field, and σ the standard deviation, or space constant, of the Gaussian. Two Gaussians, constrained to have the same sign (both on or both off), were used to assess the inhomogeneous receptive fields found in the developing LGN. Because each symmetric Gaussian has four parameters, we did not attempt to overfit the data with more than two Gaussians.

To assess the degree of orientation of some receptive fields, we then used an oriented two-dimensional Gaussian,

$$A e^{-[(u-u_0)^2 / \sigma_u^2 + (v-v_0)^2 / \sigma_v^2]},$$

where u and v are the spatial axes, rotated by the angle θ ,

$$u = \cos(\theta)x + \sin(\theta)y, \quad v = -\sin(\theta)x + \cos(\theta)y,$$

and σ_u and σ_v are the space constants of the major and minor axes.

A few cells whose receptive-field centers extended slightly beyond the edge of the monitor were used only to assess receptive-field size by fitting to a single, symmetric Gaussian. Two cells with widely spaced hot spots were very poorly fit by an elongated Gaussian. For these cells, we projected the two-dimensional spatial receptive field, along its longest and shortest axes, to produce one-dimensional profiles. The ratio of the widths of these one-dimensional profiles (at $1/e$) was taken as the aspect ratio.

To assess the goodness of fit, we calculated the mean-squared error of each model, $\frac{1}{N} \sum_{i=1}^N (R_i - M_i)^2$, where R_i is the actual value of the spatial receptive field at pixel i , and M_i is the value of the best-fit model. Comparisons between models—for instance, the two-Gaussian versus one-Gaussian—were made by taking the ratio of the mean-squared errors.

Our two methods of characterizing asymmetrical receptive fields—comparing one-versus two Gaussian fits and using elliptical fits—were only loosely correlated. The relation between them was assessed with a regression analysis of the ellipse aspect ratio (our measure of orientation; Fig. 6) against the two-Gaussian:one-Gaussian error ratio (Fig. 4d). As might be expected, there was an overall negative correlation between these two measures, one of orientation, the other of ‘bumpiness’. (The correlation was negative because the error ratio was lower for receptive fields better fit with two Gaussians.) For the entire population, the cor-

relation was fairly weak, $R^2 = 0.46$. For the 19 developing cells that were best fit by two Gaussians (error ratio < 0.75 ; see Fig. 4d), however, the two-Gaussian:one-Gaussian error ratio and the ellipse aspect ratio were completely independent ($R^2 = 0.02$).

ACKNOWLEDGEMENTS

This work was supported by NIH grants EY10115 and EY12196, The Lefler Fund and the Quan Foundation. W. Martin Usrey and John Reppas provided assistance at all stages of this project. Sergey Yurgenson provided programming assistance, and Elisabeth Serra and Christine Couture, technical assistance. Markus Meister, Kenneth Miller, John Assad, Saeed Tavazoie, Ben Gewurz and Vamsi Mootha gave comments on previous versions of this manuscript.

RECEIVED 8 DECEMBER 1999; ACCEPTED 3 APRIL 2000

- Wiesel, T. N. & Hubel, D. H. Single-cell responses in striate cortex of kittens deprived of vision in one eye. *J. Neurophysiol.* 26, 1003–1017 (1963).
- Rakic, P. Prenatal genesis of connections subserving ocular dominance in the rhesus monkey. *Nature* 261, 467–471 (1976).
- LeVay, S., Stryker, M. P. & Shatz, C. J. Ocular dominance columns and their development in layer IV of the cat's visual cortex: a quantitative study. *J. Comp. Neurol.* 179, 223–244 (1978).
- Stryker, M. P. & Harris, W. A. Binocular impulse blockade prevents the formation of ocular dominance columns in cat visual cortex. *J. Neurosci.* 6, 2117–2133 (1986).
- Katz, L. C. & Shatz, C. J. Synaptic activity and the construction of cortical circuits. *Science* 274, 1133–1138 (1996).
- Miller, K. D. A model for the development of simple cell receptive fields and the ordered arrangement of orientation columns through activity-dependent competition between ON- and OFF-center inputs. *J. Neurosci.* 14, 409–441 (1994).
- Galli, L. & Maffei, L. Spontaneous impulse activity of rat retinal ganglion cells in prenatal life. *Science* 242, 90–91 (1988).
- Meister, M., Wong, R. O., Baylor, D. A. & Shatz, C. J. Synchronous bursts of action potentials in ganglion cells of the developing mammalian retina. *Science* 252, 939–943 (1991).
- Artola, A. & Singer, W. Long-term potentiation and NMDA receptors in rat visual cortex. *Nature* 330, 649–652 (1987).
- Bear, M. F., Kleinschmidt, A., Gu, Q. A. & Singer, W. Disruption of experience-dependent synaptic modifications in striate cortex by infusion of an NMDA receptor antagonist. *J. Neurosci.* 10, 909–925 (1990).
- Mooney, R., Penn, A. A., Gallego, R. & Shatz, C. J. Thalamic relay of spontaneous retinal activity prior to vision. *Neuron* 17, 863–874 (1996).
- Bienenstock, E. L., Cooper, L. N. & Munro, P. W. Theory for the development of neuron selectivity: orientation specificity and binocular interaction in visual cortex. *J. Neurosci.* 2, 32–48 (1982).
- Von der Malsburg, C. & Cowan, J. D. Outline of a theory for the ontogenesis of iso-orientation domains in visual cortex. *Biol. Cybern.* 45, 49–56 (1982).
- Daniels, J. D., Pettigrew, J. D. & Norman, J. L. Development of single-neuron responses in kitten's lateral geniculate nucleus. *J. Neurophysiol.* 41, 1373–1393 (1978).
- Blakemore, C. & Vital-Durand, F. Organization and post-natal development of the monkey's lateral geniculate nucleus. *J. Physiol. (Lond.)* 380, 453–491 (1986).
- Mason, C. A. Development of terminal arbors of retino-geniculate axons in the kitten—I. Light microscopical observations. *Neuroscience* 7, 541–559 (1982).
- Sur, M., Weller, R. E. & Sherman, S. M. Development of X- and Y-cell retinogeniculate terminations in kittens. *Nature* 310, 246–249 (1984).
- Sretavan, D. W. & Shatz, C. J. Prenatal development of retinal ganglion cell axons: segregation into eye-specific layers within the cat's lateral geniculate nucleus. *J. Neurosci.* 6, 234–251 (1986).
- Tootle, J. S. & Friedlander, M. J. Postnatal development of the spatial contrast sensitivity of X- and Y-cells in the kitten retinogeniculate pathway. *J. Neurosci.* 9, 1325–1340 (1989).
- Barlow, H. B. & Pettigrew, J. D. Lack of specificity of neurones in the visual cortex of young kittens. *J. Physiol. (Lond.)* 218, 98–100 (1971).
- Albus, K. & Wolf, W. Early post-natal development of neuronal function in the kitten's visual cortex: a laminar analysis. *J. Physiol. (Lond.)* 348, 153–185 (1984).
- Chapman, B. & Stryker, M. P. Development of orientation selectivity in ferret visual cortex and effects of deprivation. *J. Neurosci.* 13, 5251–5262 (1993).
- Chapman, B., Stryker, M. P. & Bonhoeffer, T. Development of orientation preference maps in ferret primary visual cortex. *J. Neurosci.* 16, 6443–6453 (1996).
- Gödecke, I., Kim, D. S., Bonhoeffer, T. & Singer, W. Development of orientation preference maps in area 18 of kitten visual cortex. *Eur. J. Neurosci.* 9, 1754–1762 (1997).
- Issa, N. P., Trachtenberg, J. T., Chapman, B., Zahs, K. R. & Stryker, M. P. The critical period for ocular dominance plasticity in the ferret's visual cortex. *J. Neurosci.* 19, 6965–6978 (1999).
- Reid, R. C., Victor, J. D. & Shapley, R. M. The use of m-sequences in the analysis of visual neurons: linear receptive field properties. *Vis. Neurosci.* 14, 1015–1027 (1997).
- Hubel, D. H. & Wiesel, T. N. Integrative action in the cat's lateral geniculate body. *J. Physiol. (Lond.)* 155, 385–398 (1961).
- Vidyasagar, T. R. & Urbas, J. V. Orientation sensitivity of cat LGN neurones with and without inputs from visual cortical areas 17 and 18. *Exp. Brain Res.* 46, 157–169 (1982).
- Soodak, R. E., Shapley, R. M. & Kaplan, E. Linear mechanism of orientation tuning in the retina and lateral geniculate nucleus of the cat. *J. Neurophysiol.* 58, 267–275 (1987).
- Cleland, B. G., Dubin, M. W. & Levick, W. R. Simultaneous recording of input and output of lateral geniculate neurones. *Nat. New Biol.* 231, 191–192 (1971).
- Usrey, W. M., Reppas, J. B. & Reid, R. C. Specificity and strength of retinogeniculate connections. *J. Neurophysiol.* 82, 3527–3540 (1999).
- Hammond, P. Cat retinal ganglion cells: size and shape of receptive field centres. *J. Physiol. (Lond.)* 242, 99–118 (1974).
- Cai, D., DeAngelis, G. C. & Freeman, R. D. Spatiotemporal receptive field organization in the lateral geniculate nucleus of cats and kittens. *J. Neurophysiol.* 78, 1045–1061 (1997).
- Murphy, P. C. & Sillito, A. M. Corticofugal feedback influences the generation of length tuning in the visual pathway. *Nature* 329, 727–729 (1987).
- Sherman, S. M. & Guillery, R. W. On the actions that one nerve cell can have on another: distinguishing “drivers” from “modulators”. *Proc. Natl. Acad. Sci. USA* 95, 7121–7126 (1998).
- Hamos, J. E., Van Horn, S. C., Raczkowski, D., Uhlrich, D. J. & Sherman, S. M. Synaptic connectivity of a local circuit neurone in lateral geniculate nucleus of the cat. *Nature* 317, 618–621 (1985).
- Alonso, J. M., Usrey, W. M. & Reid, R. C. Precisely correlated firing in cells of the lateral geniculate nucleus. *Nature* 383, 815–819 (1996).
- Usrey, W. M., Reppas, J. B. & Reid, R. C. Paired-spike interactions and synaptic efficacy of retinal inputs to the thalamus. *Nature* 396, 384–387 (1998).
- Cleland, B. G. in *Visual Neuroscience* (eds Pettigrew, J. D., Sanderson, K. S. & Levick, W. R.) 111–120 (Cambridge Univ. Press, London, 1986).
- Mastroratte, D. N. Interactions between ganglion cells in cat retina. *J. Neurophysiol.* 49, 350–365 (1983).
- Henderson, Z., Finlay, B. L. & Wikler, K. C. Development of ganglion cell topography in ferret retina. *J. Neurosci.* 8, 1194–1205 (1988).
- Linden, D. C., Guillery, R. W. & Cucchiari, J. The dorsal lateral geniculate nucleus of the normal ferret and its postnatal development. *J. Comp. Neurol.* 203, 189–211 (1981).
- Peters, A. & Payne, B. R. Numerical relationships between geniculocortical afferents and pyramidal cell modules in cat primary visual cortex. *Cereb. Cortex* 3, 69–78 (1993).
- Peichl, L. & Wässle, H. Size, scatter and coverage of ganglion cell receptive field centres in the cat retina. *J. Physiol. (Lond.)* 291, 117–141 (1979).
- Kirkwood, A., Lee, H. K. & Bear, M. F. Co-regulation of long-term potentiation and experience-dependent synaptic plasticity in visual cortex by age and experience. *Nature* 375, 328–331 (1995).
- Reid, R. C. & Alonso, J. M. Specificity of monosynaptic connections from thalamus to visual cortex. *Nature* 378, 281–284 (1995).
- Crowley, J. C. & Katz, L. C. Development of ocular dominance columns in the absence of retinal input. *Nat. Neurosci.* 2, 1125–1130 (1999).
- Sherk, H. & Stryker, M. P. Quantitative study of cortical orientation selectivity in visually inexperienced kitten. *J. Neurophysiol.* 39, 63–70 (1976).
- Zahs, K. R. & Stryker, M. P. The projection of the visual field onto the lateral geniculate nucleus of the ferret. *J. Comp. Neurol.* 241, 210–224 (1985).
- Price, D. J. & Morgan, J. E. Spatial properties of neurones in the lateral geniculate nucleus of the pigmented ferret. *Exp. Brain Res.* 68, 28–36 (1987).